ISSN: 2572-3235

Mourão et al. Int J Radiol Imaging Technol 2019, 5:050
DOI: 10.23937/2572-3235.1510050
Volume 5 | Issue 1
Open Access

International Journal of
Radiology and Imaging Technology

ORIGINAL ARTICLE

Dosimetry and Protocol Optimization of Computed Tomography Scans using Adult Chest Phantoms

Arnaldo Prata Mourão[1,2], Wadia Namen Aburjaile, Phd[1] and Fernanda Stephanie Santos[1]*

[1]*Department of Nuclear Engineering, Federal University of Minas Gerais, Brazil*

[2]*Center of Biomedical Engineering, Federal Center for Technological Education of Minas Gerais, Brazil*

***Corresponding author:** *Arnaldo Prata Mourão, Department of Nuclear Engineering, Federal University of Minas Gerais, Belo Horizonte, Brazil: Center of Biomedical Engineering, Federal Center for Technological Education of Minas Gerais, Belo Horizonte, Brazil*

Abstract

Computed Tomography (CT) has become an important tool for diagnosing cancer and to obtain additional information on different clinical issues. The radiation dose values in computed tomography depend on the scan acquisition protocol. Today, it is a very fast, painless and noninvasive test that can be performed high quality images. Therefore, it is indispensable to improve protocols, seeking smaller doses, without impairing the diagnostic quality of the image. The doses received are related with risks of stochastic effects. Based on this information, in this study, a cylindrical phantom and an oblong phantom made of polymethylmethacrylate were used representing an adult chest, The oblong phantom was built based in the chest cut section, including axillary region, with the same cut area of the cylindrical phantom. A comparative study of chest phantoms was performed in a Toshiba scanner, Aquillion model with 80 channels. The phantom central slice has been irradiated successively, and measurements in five different points of each phantom have done using a pencil ionization chamber. From the measurements, we obtain values of weighted and volumetric Dose Index (CTD_{lw}, CTD_{lvol}). The scans have been performed with the routine chest acquisition protocols of the radio diagnostic service with the voltage of 120 kV and additionally with the voltage of 135 kV. This study has allowed comparing the distribution of absorbed dose in two phantoms using two different voltages.

Keywords

Computed tomography, Human phantoms, Dosimetry, Chest CT scans

Introduction

Computed tomography devices currently installed in radio diagnostic services present wide technological variations. Thus, images generated with the same diagnostic objective in different devices can generate different doses in patient, very different, either by the technological difference or the acquisition protocol used [1,2].

The ionizing radiation originated from the X-rays used for diagnosis is the artificial source that contributes most to the exposure dose of the population due to the large number of X-ray examinations performed per year. Computed Tomography tests are the radio diagnostic examination that contributes most to the dose increase in the population [2,3].

For the year 2006, the contribution of medical exposures in the composition of the effective population in the USA corresponds to 48%, with 24% due to CT examinations. The other 52% coming from other sources such: As Radon 37%, spatial origin 5%, terrestrial 3% and internal 5%. Considering this data, it can be estimated that currently this population receives practically twice the dose received before the discovery of X-rays [4]. With this, there is a growing concern of the medical community, equipment manufacturers and even patients regarding the control of the dose of radiation determined by the various tests that use ionizing radiation [5,6].

Several factors contribute to the increased demand for CT scans, including the constant technological evolution of the equipment associated to greater availabil-

Citation: Mourão AP, Aburjaile WN, Santos FS (2019) Dosimetry and Protocol Optimization of Computed Tomography Scans using Adult Chest Phantoms. Int J Radiol Imaging Technol 5:050. doi.org/10.23937/2572-3235.1510050

Accepted: June 20, 2019: **Published:** June 22, 2019

ity and a relative tendency to decrease exam costs. The risks of stochastic effects increase with the absorbed dose and the deposited dose in patient is directly related to the energy that was retained during the process of exposure to ionizing radiation [1,5,7].

The knowledge of the dose distribution is important when one thinks of varying the acquisition parameters aiming its reduction. For these reasons, there is a growing concern about the radiation dose used in radiological exams, especially CT scans, to address actions to reduce the doses. CT scans result in absorbed doses in organs in the range of 10 to 100 mGy, usually below the lower limit considered for the occurrence of deterministic effects [1,8,9].

However, all procedures involving ionizing radiation can lead to stochastic effects, such as tumor induction. The manufacturers have introduced several actions, for example: Specific protocols for pediatric patients, current modulation in the organ-based tube and interactive reconstruction [10,11].

In this work it was used two different chest adult phantoms to observe the dose distribution and to obtain the dose index. Different protocols were used in the phantom CT scans using two X-ray tube voltages [12-14].

Materials and Methods

The CT scans were performed using two acquisition protocols and two different adult chest phantoms. Absorbed doses were recorded in five different points in both phantoms to obtain the index dose values.

Table 1: Characteristics of CT scanner.

Brand	Model	Channels	Voltage (kV)	Beam Thickness (mm)
Toshiba	Aquillion	80	120, 135	40

Computed tomography device

The experiments for the observation and comparison of the CT air kerma index and CT dose index on the chest phantoms have carried out on a multislice CT Toshiba scanner, Aquillion model with 80 channels. To capture data on the absorbed doses, it has used two different acquisition protocols. Table 1, shows the main characteristics of the CT scanner used.

Phantoms

The team of the Center for Research in Biomedical Engineering (CENEB) of the Federal Center for Technological Education of Minas Gerais (CEFET-MG) has built two chest phantoms by the research, both representative of an adult chest. The first phantom is a cylinder made of PMMA with 32 cm in diameter and 15 cm in length. This phantom is the default for the dose reference in chest CT scans. Thus, all chest CT scans performed are accompanied by a report that presents a dose estimated value by the CT scanner software ($CTDI_{vol}$) based on the scanning of this phantom [8,11].

The second chest phantom made of PMMA is oblong with dimensions of 43 cm in width and 22 cm in height. The cut area of the oblong phantom is defined by two semi ellipses generated from an ellipse of 30 cm by 22 cm and a rectangle of 22 cm by 13 cm. It was developed based on the size of the chest, in axillary region of an adult human body. This oblong chest phantom has the same surface area of the cylindrical phantom and the same length of 15 cm, and therefore, the same volume of the cylindrical phantom. Figure 1 shows an image of the two phantoms placed in isocenter of the gantry CT scanner.

The phantoms have five openings for positioning dosimeters, one central being representative of the

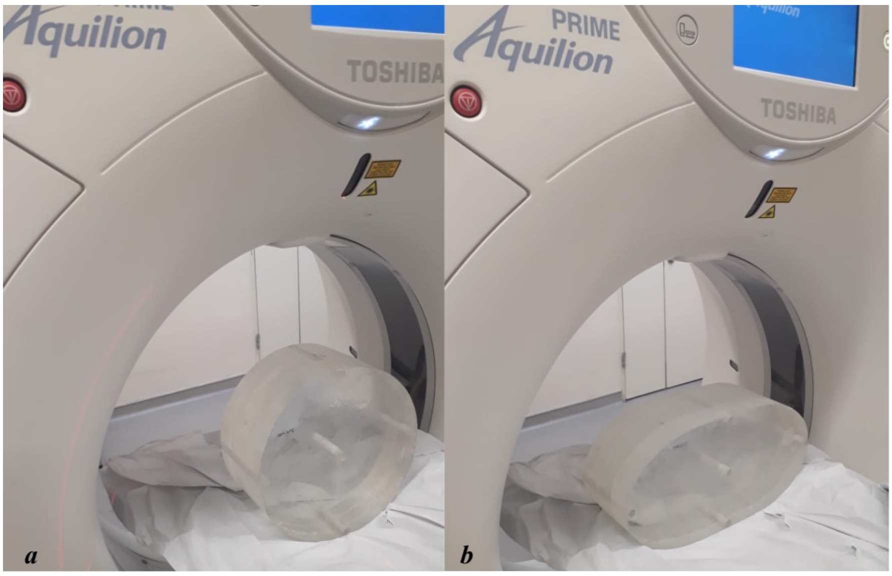

Figure 1: Images of PMMA chest phantoms, cylindrical (a) and oblong (b), placed in the CT scanner.

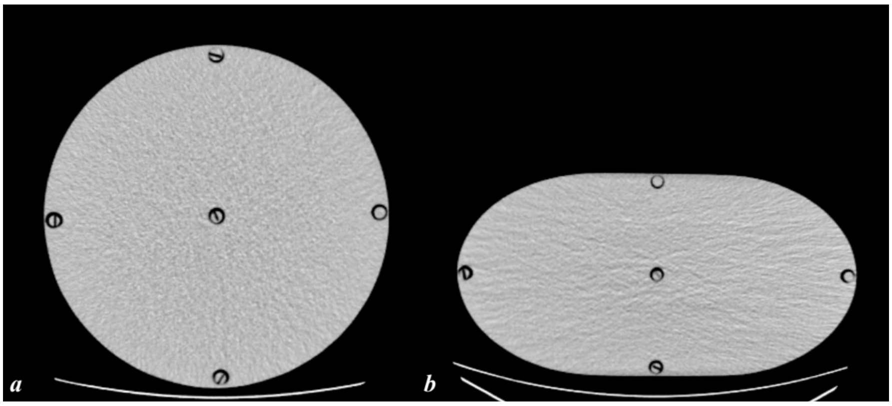

Figure 2: Axial cutting images of the phantom central slice with positions measurements in cylindrical (a) and oblong (b) phantoms.

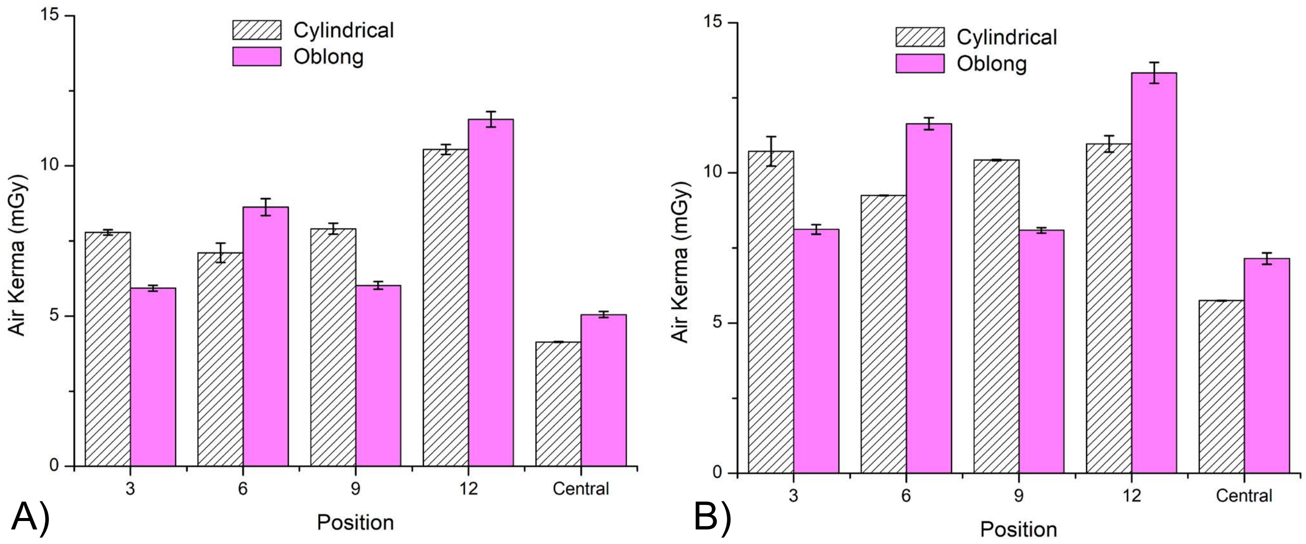

Figure 3: Graphics of $C_{k,PMMA,100}$, for 100 mAs 120 kV (a) and 135 kV (b) voltages.

Table 2: CT acquisition axial protocols.

Protocol	Voltage (kV)	Current (mA)	Time (s)	Charge (mA.s)	Beam Thickness (mm)
I	135	200	0.5	100	10
II	120	200	0.5	100	10

mediastinum and four peripheral positions of 12.7 mm in diameter and 15 cm in length. The four peripheral openings are 90° out of phase, the center of which is 10 mm from the phantom edge. In analogy to the display of an analog clock, peripheral openings were named 3, 6, 9 and 12, according to position within the gantry during the scanning of the central slice [2,8]. In relation to anatomical structures, positions 3 and 9 correspond to the axillary regions. The positions 6 and 12 correspond to the thoracic spine and sternal bone, respectively. These positions of measurement allow observing the dose deposition variations. Figure 2 shows axial cutting images of the cylindrical and oblong phantoms.

To perform the CT scans, the phantoms were positioned in the isocenter of the gantry, and the peripheral openings were used for the phantom alignment with the aid of the lights of the gantry laser lights. Figure 3 shows the positioning of the cylindrical phantom in the gantry isocenter.

Dose measurements

The phantom openings are filled with PMMA rods, which must be removed one by one for the positioning of the pencil chamber, targeting the measurements in the five positions. Air Kerma in PMMA ($C_{k,100P,MMA}$) was performed using a RADCAL ACCU-GOLD dosimetry set with a pencil ionizing chamber model 10 × 6-3CT. The protocol used to irradiate the central slice is presented in Table 2 [12,15].

The measurements obtained ($C_{k,100,PMMA}$) were converted to CT dose index ($CTDI_{100}$) using a ratio of 1.042 and 1.045 based on the proportion of attenuation coefficients PMMA/air [16-18].

Table 3: Acquisition helical protocols used in CT scans.

Phantom	Protocol	Voltage (kV)	Average Current (mA)	Charge (mA.s)
Cylindrical	I	120	500	250
	II	135	420	210
Oblong	I	120	424	232
	II	135	380	190

Table 4: Values of $C_{k,PMMA,100}$ in mGy and standard deviation for adult chest phantoms.

Phantom	Voltage kV		Position				
			3	6	9	12	Central
Cylindrical	120	Value	7.79	7.11	7.91	10.55	4.14
		SD	0.09	0.32	0.18	0.16	0.01
	135	Value	10.72	9.25	10.43	10.97	5.75
		SD	0.49	0.01	0.02	0.27	0.01
Oblong	120	Value	5.93	8.63	6.02	11.55	5.05
		SD	0.10	0.28	0.13	0.26	0.10
	135	Value	8.12	11.64	8.09	13.33	7.15
		SD	0.16	0.20	0.09	0.35	0.19

Scanning protocols

In the examination room, the adult phantoms have been placed on the table and, with the aid of laser lights; they were oriented so that their central axis passed through the isocenter of the gantry during the table displacement [19,20]. They central area of the phantoms were scanned in helical mode with voltages of 120 and 135 kV using the system automatic control, electrical current in automatic, in the rage of 50 to 500 mA [12,13,20]. The scan distance was 10 cm, with pitch of 1,388 using 80 detectors of 0.5 mm. The CT Table 3 shows the others protocol parameters used in the scans realized in both phantoms. The chosen parameters were based on the routine protocol used by the service voltage of 120 kV, automatic current, tube time of 0.5 s, detector length of 80 × 0.5 cm and pitch of 1.388.

Dose index values

The values of air kerma in PMMA ($C_{k,PMMA,100}$) are obtained by reading the values recorded on the electrometer duly calibrated by the influence of temperature and pressure. In order to obtain the weighted index ($C_{k,w}$) it was used the equation 1 and to obtain the volumetric index ($C_{k,vol}$) it was used the equation 2. Dose values were obtained using the conversion factors of PMMA and air according with the voltage (1.042 and 1.045) [1,2,17,18].

$$C_{k,\,w} = \frac{1}{3} C_{k,\,100,\,central} + \frac{2}{3} ck, 100,\, peripheral$$

$$C_{k,\,vol} = \frac{C_{k,w}}{pitch}$$

Results

Measurements of $C_{k,PMMA,100}$

It has done the irradiation of the central slice of the adult phantoms using the parameters defined in Table 2. The average values obtained for each position and the standard deviation (SD) of the measurement are presented in the Table 4. In observation of the average values recorded in the five positions, it is verified that, among the values of air kerma recorded, the highest value was 13.33 ± 0.35 mGy, and it occurred in position 12 with 135 kV of the oblong phantom, and the lowest was 4.14 ± 0.01 mGy in the central position of the cylindrical phantom with 120 kV.

The proximity between the doses in points 3 and 9 indicates the good positioning of the object in the isocenter of the gantry. It should be noted that the dose recorded in points 3 and 9 are important, since there are located axillary lymphatic chains that are radiosensitive. The Figure 3 shows graphics of $C_{k,PMMA,100}$ values for adult phantoms using 100 mAs and 120 kV in *a* and 100 mAs and 135 kV in b.

Dose indexes

The values of the indexes $C_{k,w}$, $C_{k,vol}$ and $CTDI_{vol}$ are presented in the Table 5. The values were adjusted using the average current, the pitch value and the correction fator PMMA/air.

The Figure 4 shows graphics of $CTDI_{VOL}$ values for adult phantoms obtained according with the average current and pitch.

The average values obtained for each position and the standard deviation (SD) of the measurement are in the Table 4. For the average values recorded in the five positions, it is verified that, among the values of air kerma recorded, the highest value was 13.33 ± 0.35 mGy, and it occurred in position 12 with 135 kV of the oblong phantom, and the lowest was 4.14 ± 0.01 mGy in the central position of the cylindrical phantom with 120 kV.

DOI: 10.23937/2572-3235.1510050 ISSN: 2572-3235

Table 5: Values of $C_{k,w,}$ $C_{k,vol}$ and $CTDI_{vol}$ in mGy for adult chest phantoms.

Phantom	Voltage kV		Index		
			$C_{k,w}$	$C_{k,vol}$	$CTDI_{VOL}$
Cylindrical	120	Value	17.35	12.50	13.02
		SD	0.32	0.23	0.24
	135	Value	18.50	13.33	13.93
		SD	0.28	0.20	0.21
Oblong	120	Value	16.33	11.77	12.26
		SD	0.37	0.27	0.28
	135	Value	17.56	12.65	13.22
		SD	0.38	0.27	0.28

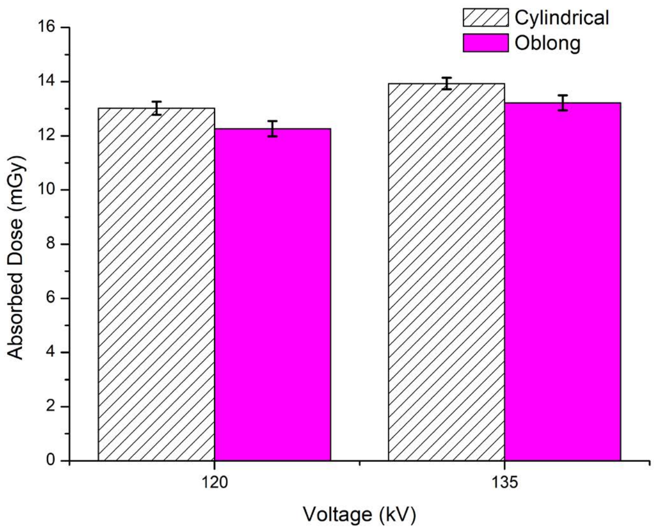

Figure 4: Graphics of $CTDI_{VOL}$ for 120 and 135 kV.

Discussion

The use of phantoms is important to understand the spatial dose distribution. The graphics in Figure 3a and Figure 3b use the same current value (200 mA) and they show that the oblong phantom receive higher doses than the cylindrical phantom in the positions: 6 (spine), central (mediastinum) and 12 (sternal bone) where the phantom have a smaller thickness. This situation can happen when it is used a same protocol and the current automatic control is not activated. It is important to know that some CT scanners don't have the possibility of the use this tool and sometimes this tool is not activated by the protocols existent in the equipment.

The use of 135 kV voltage and the same current (200 mA) promoted the deposition of higher doses, because X-ray beams more energetic deposit more dose. However, it's important to verify that the use of a more energetic beam promotes the same behavior for all positions in the dose deposition in the phantoms. Higher doses happened in the positions 6, 12 and central of the oblong phantom.

The use of the automatic current control promotes lower currents in the oblong phantom CT scans than in the cylindrical phantom, 9.52% for the 120 kV protocol and 15.2% for the 135 kV. This situation is demonstrate in the values of the $CTDI_{vol}$ presented in the Figure 4, in the oblong phantom is 5.8% smaller for the 120 kV protocol, and 5.1% for the 135 kV.

The protocol of 120 kV generated smaller absorbed doses in both phantoms. However is important to know that the average current value used in the cylindrical phantom, for the voltage of 120 kV, reached the maximum limit of 500 mA. This limitation promoted the generation of images with a little higher noise. The standard deviation of the ROI observed in the central slice image was 18.69 HU (Hounsfield unit) and in the oblong phantom was 15.25 HU, corresponding a noise of 1.67% and 1.36%, respectively. This situation could indicate that the current for the cylindrical phantom should be higher than 500 mA in the use of 120 kV.

Conclusion

The developed oblong chest phantom allowed the verification of how the dose distribution can vary with the object shapes with the same volume. When comparing with the data obtained for the standard adult chest phantom, it was found that doses in the oblong phantom have been higher in the vertical axis positions.

The use of oblong chest phantom has shown that the use of automatic current control promotes lower doses in this phantom in both protocols. So, the use of this tool is really important in areas where thickness variations exist in the cut area.

The use of the lower voltage (120 kV) generated smaller dose in CT scans for both phantoms. But the use of the maximum limit current (500 mA) could indicate that in higher volumes the use of the 135 kV can be better to improve the image quality.

Acknowledgments

This work was supported by the FAPEMIG, CAPES and the Metropolitan Hospital.

References

1. Pernicka F, McLean ID (2007) Dosimetry in diagnostic radiology: An international code of practice. International Atomic Energy Agency.
2. Mourão AP, Alonso TC, DaSilva TA (2014) Dose profile variation with voltage in head CT scans using radiochromic films. Radiation Physics and Chemistry 95: 254-257.
3. Kleinman PL, Strauss KJ, Zurakowski D, Buckley KS, Taylor GA (2010) Patient size measured on CT images as a function of age at a tertiary care children's hospital. AJR 194: 1611-1619.
4. Bolus NE (2013) NCRP report 160 and what it means for medical imaging and nuclear medicine. J Nucl Med Technol 41: 255-260.
5. Mourão AP (2015) Tomografia Computadorizada: Tecnologias e aplicações. São Caetano do Sul: Difusao.
6. (1996) International basic safety standards for protection against ionizing radiation and for safety of radiation sources. International Atomic Energy Agency, Safety Series. 115, Vienna, Austria.
7. Calzado A, Geleijns J (2010) Tomografía computarizada. Evolución, principios técnicos y aplicaciones. Rev Fís Méd 11: 163-180.
8. (2010) Comprehensive methodology for the evaluation of radiation dose in X-Ray computed tomography. AAPM Report No. 111, Maryland.
9. Nakayama Y, Awai K, Funama Y, Hatemura M, Imuta M, et al. (2005) Abdominal CT with low tube voltage: Preliminary observations about radiation dose, contrast enhancement, image quality, and noise. Radiology 237: 945-951.
10. Aburjaile WN, Mourao AP (2017) Development of a chest phantom for testing in computed tomography scans. Radiation Physics and Chemistry 140: 275-277.
11. Alonso TC, Mourão AP, Santana PC, da Silva TA (2016) Assessment of breast absorbed doses during thoracic computed tomography scan to evaluate the effectiveness of bismuth shielding. Appl Radiat Isot 117: 55-57.
12. Sakhnini L (2017) CT radiation dose optimization and reduction for routine head, chest and abdominal CT examination. Radiol Diagn Imaging 2: 1-4.
13. Thakur Y, McLaughlin PD, Mayo JR (2013) Strategies for radiation dose optimization. Current Radiology Reports 1: 1-10.
14. (2012) Quality Assurance programme for Computed Tomography: Diagnostic and Therapy Applications. IAEA Human Health Series No. 19.
15. Bauhs JA, Vrieze TJ, Primak AN, Bruesewitz MR, McCollough CH (2008) CT dosimetry: Comparison of measurement techniques and devices. Radiographics 28: 245-253.
16. Gómez AML (2017) Estudo de dosimetria e qualidade de imagem em varreduras de tomografia computadorizada de cabeça utilizando objeto simulador. Master Dissertation Federal University of Minas Gerais, Belo Horizonte, Brazil.
17. (2017) National Institute of Standards and Technology.
18. Duan X, Wang J, Yu L, Leng S, McCollough CH (2011) CT scanner x-ray spectrum estimation from transmission measurements. Med Phys 38: 993-997.
19. Khan AN, Shuaib W, Nikolic B, Khan MK, Kang J, et al. (2014) Absorbed radiation dose in radiosensitive organs using 64-and 320-row multidetector computed tomography: A comparative study. Scientifica
20. Kanal KM, Stewart BK, Kolokythas O, Shuman WP (2007) Impact of operator-selected image noise index and reconstruction slice thickness on patient radiation dose in 64-MDCT. AJR Am J Roentgenol 189: 219-225.